Does humidity matter? Prenatal heat and child health in South Asia

Kathryn McMahon[1,*], Kathy Baylis[1], Stuart Sweeney[1], and Chris Funk[2]

[1]Department of Geography, University of California, Santa Barbara, Santa Barbara, CA 93106
[2]Climate Hazards Center, University of California, Santa Barbara, Santa Barbara, CA 93106
[*]kathryn.mcmahon@geog.ucsb.edu

ABSTRACT

Heat extremes pose significant health risks during pregnancy and early childhood. High humidity exacerbates heat stress but is overlooked by existing models. We investigate the influence of prenatal heat and humidity extremes on child health in South Asia, a region with a high prevalence of child stunting and rapidly increasing hot-humid extremes. After controlling for sociodemographic factors, seasonality, and time period, we exploit within-village variation in children's ages to isolate the effect of prenatal heat exposure. We find that hot-humid heat is much more detrimental to child health than hot temperatures alone. Our results suggest that increasing heat and humidity from climate change could drive over 2.2 million additional children in the region into stunting by 2050, a four-fold increase relative to the temperature-only model. These findings underscore the importance of accounting for both temperature and humidity when estimating climate change impacts, particularly in vulnerable regions like South Asia.

Due to climate change, extreme heat events are increasing in frequency, intensity, and duration, posing an immediate and growing threat to human health[1]. While the scientific literature has largely focused on the important issue of heat-related mortality[2–4], the lasting health impacts of heat on the living are often overlooked, despite growing evidence linking extremes with higher morbidity[5–7]. Even in healthy adults, prolonged exposure to hot environments can raise body temperatures to dangerous levels, straining the heart and increasing rates of both temporary and permanent organ damage, particularly for the kidneys[5,6]. High humidity exacerbates these effects by preventing the evaporation of sweat from our skin, inhibiting the body's natural cooling mechanism[8]. Ambient air temperature is therefore a coarse measure of the biological stress associated with heat exposure, which is better captured by composite metrics like the wet-bulb globe temperature that account for the additional factors that lead to heat stress[9,10]. While temperature and humidity are critical factors, wet-bulb globe temperature and related metrics also incorporate characteristics like wind speed, cloud cover, and sunlight intensity. When we focus only on the impacts of air temperature, we may considerably underestimate the true cost of climate change, especially in the hot and humid global tropics[11].

Pregnant people and their babies are at a heightened risk for the health consequences associated with hot-humid environments. During pregnancy, changing hormone levels and increased metabolic heat production inhibit natural cooling, making maternal core temperature more sensitive to the effects of hot-humid heat and increasing the risk of maternal heat stress, pregnancy loss, and complications at birth[12–14]. One multi-national study in sub-Saharan Africa finds that mean birth weights fall by up to 0.9 grams for each day during pregnancy where temperatures reach 100°F (38°C)[15], while another finds that a 10% increase in the number of days over 104°F (40°C) raises the likelihood of late-stage pregnancy loss by 1.9%[16]. Given recent advancements in gridded temperature data[17,18] and an increasing understanding of the importance of additional environmental factors like humidity[19], these studies may underestimate the true effect of extreme heat. In addition to undermining infant health at birth, prenatal exposures also threaten long-term wellbeing. Disruptions to health and nutrition during the first 1,000 days after conception have been quantifiably linked to educational, financial, and physical outcomes well into adulthood[20–23].

Social and physical vulnerability to extreme heat intersect in South Asia, where inequalities in resource access and high rates of child undernutrition come head-to-head with rapidly accelerating exposure to extreme heat and humidity[24,25]. Now and in the future, hot-humid conditions are concentrated along South Asia's river valleys and coasts, which are also home to some of the densest populations in the world (SI Fig. 1;[26]). Even if societies succeed in limiting warming to 2°C above preindustrial levels, South Asia is expected to suffer from deadly heat events every year[27]. Meanwhile, rates of child stunting remain high throughout the region. In 2023, the United Nation's Children's Fund (UNICEF) reported that South Asia was home to one third (54 million) of the world's stunted children[28]. Furthermore, existing research shows that the burdens of child undernutrition and climate change are intrinsically intertwined. Nutritional status is highly sensitive to environmental shocks up to age 5[29], particularly for children in poor households who often lack the social and material resources necessary for shock mitigation and

recovery[30–32].

In this paper, we conduct a spatially-granular analysis of the effects of prenatal exposure to extreme heat and humidity on height attainment for approximately 200,000 children in Bangladesh, India, and Nepal. After controlling for a comprehensive set of demographic characteristics and spatio-temporal confounders related to nutrition, we utilize short-run variation in daily maximum temperature (Tmax) and maximum wet-bulb globe temperature (WBGTmax) to observe the effect of heat extremes on height-for-age Z-scores (HAZ) in children under the age of five, a key indicator of chronic undernutrition at a critical stage of growth and development. Our design adjusts for the non-random assignment of heat exposure across our sample from spatial and seasonal factors using a village-level fixed effect, a state-by-survey year fixed effect, and controlling for childrens' calendar month of birth. We therefore compare children with similar sociodemographic characteristics who were born in the same community and calendar month but slightly different years, which provides plausibly exogenous variation in the weather conditions during their prenatal periods. When we define extreme heat using WBGTmax, a heat stress metric that incorporates humidity, we find that prenatal heat exposure is more detrimental to child growth than when we estimate this relationship using temperature alone. Specifically, a one standard-deviation increase in the number of hot-humid days in the third trimester decreases height-for-age by 3.7%. The corresponding decrease for just hot days would be 1.3%. Combined with new heat projections, our coefficient estimates on WBGTmax exposure imply that more than 2.2 million additional children would have been stunted across our study region had they been exposed to the levels of heat and humidity that are expected by 2050 under a high-emissions climate change scenario. This estimate shrinks to 500,000 additional children when we apply the coefficient estimates on maximum temperature.

To our knowledge, this study is the first to quantify the combined effects of extreme heat and humidity on child health at the regional level. Previous scholars have (1) identified children under five as a population that is particularly vulnerable to climate shocks[32–35] and (2) documented a strong link between extreme heat exposure and increased mortality, particularly for older adults[2,4,36,37], but the observed impacts of temperature extremes on morbidity and its associated economic outcomes[7] have been overlooked in the scientific literature thus far. Extreme heat harms many more people than it kills, and these lingering impacts have as-of-yet received little attention. Our findings shed light on this relationship, providing striking new evidence that humid heat events pose a large and growing threat to long-term health and economic stability for children in the global tropics.

Results

Heat Exposure

Figure 1 describes the average conditions during the nine months before birth for children in each community surveyed by the Demographic and Health Surveys (DHS). Each point represents a DHS survey location, or "cluster." These conditions are depicted in four ways: Panel (a) shows the average percentage of total days during pregnancy that were relatively cool and dry, exceeding neither heat threshold; Panel (b) shows the corresponding percentage of days that exceeded both thresholds; Panel (c) shows the percent of days where Tmax exceeded 35°C but WBGTmax stayed below 29°C, indicating dry heat; and Panel (d) shows the percent of days with WBGTmax>29°C but Tmax<35°C, suggesting warm temperatures with high humidity.

Figure 1 reveals that children born in Central Southern India and the high-elevation regions in Nepal and Northern and Eastern India experienced relatively cool and dry conditions in utero. On the other hand, children along the Southeast coast of India and the Northwest border with Pakistan–historically hot areas–were frequently exposed to days that were extremely hot by both definitions. Days in this most extreme category comprised up to 50% of the average pregnancy (or 135-140 days) in some survey locations. Finally, while hot and dry days are most common in the central swaths of the region (Panel c), those exceeding only our WBGTmax threshold (Panel d) are more concentrated along the coast of the subcontinent where humidity is relatively high, as well as in the Indian foothills of the Himalayas and much of Bangladesh. Importantly, these low, humid areas along the Ganges and Brahmaputra rivers are home to very dense populations, thus amplifying human exposure to humid heat extremes (SI Fig. 1).

The differences in spatial distribution between Panels (c) and (d) suggest considerable variation in the sub-populations that are exposed to hot versus hot-humid heat. Our subsequent analyses will explore this variation further by quantifying the relationship between child health and exposure to both heat extremes. The frequency of extreme days is largely consistent between Tmax and WBGTmax, and the distributions of each exhibit notable left-skewness (see Fig. 3). See SI Table 1 for summary statistics on heat exposure across trimesters and heat variables. Additional exploratory analyses reveal that there is a moderate positive correlation between the number of days with Tmax>35°C and WBGTmax>29°C (Pearson coefficient = 0.67) at the trimester level.

Effects on Height-for-Age

Figure 2 presents the coefficients and 95% confidence intervals on prenatal heat exposure from our main models of HAZ, estimated using a comprehensive suite of fixed effects and demographic controls (see SI for full regression results tables). Panels (a) and (b) show the coefficients on heat exposure estimated from our Tmax-only and WBGTmax-only models, respectively,

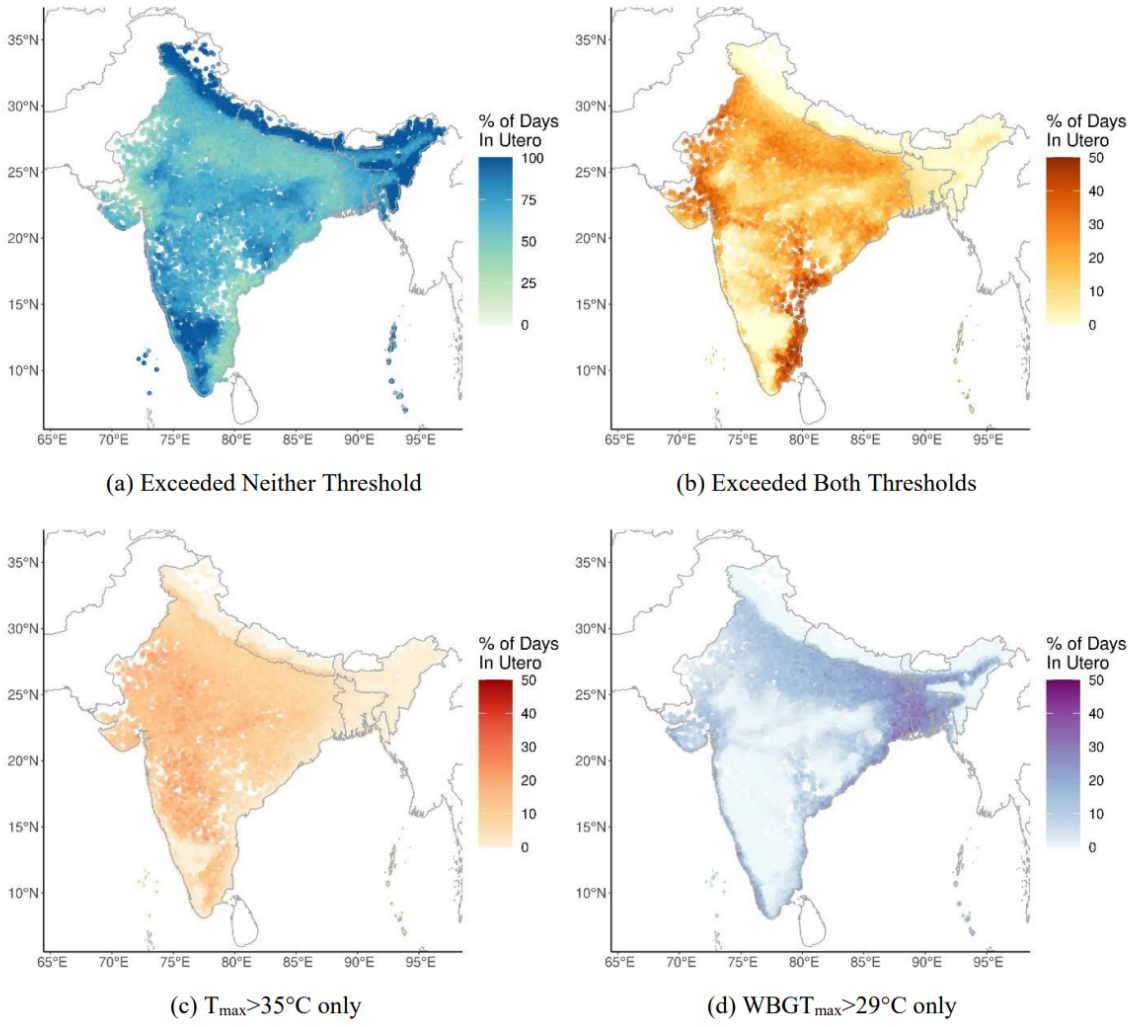

(a) Exceeded Neither Threshold

(b) Exceeded Both Thresholds

(c) T_{max}>35°C only

(d) $WBGT_{max}$>29°C only

Figure 1. Spatial distribution of prenatal heat exposure in South Asia. Each point represents a cluster (N=29,357) from the Demographic and Health Surveys, where color is determined by the average number of days in each heat category experienced during trimesters 1-3 by 0-to-5 year olds in each cluster. Panel (a) shows the percentage of total days that exceeded neither heat threshold, Panel (b) shows the percent of days that were extreme by both definitions, Panel (c) shows the percent of days that met Tmax>35°C but not WBGTmax>29°C, and Panel (d) shows the percentage with WBGTmax>29°C but not Tmax>35°C.

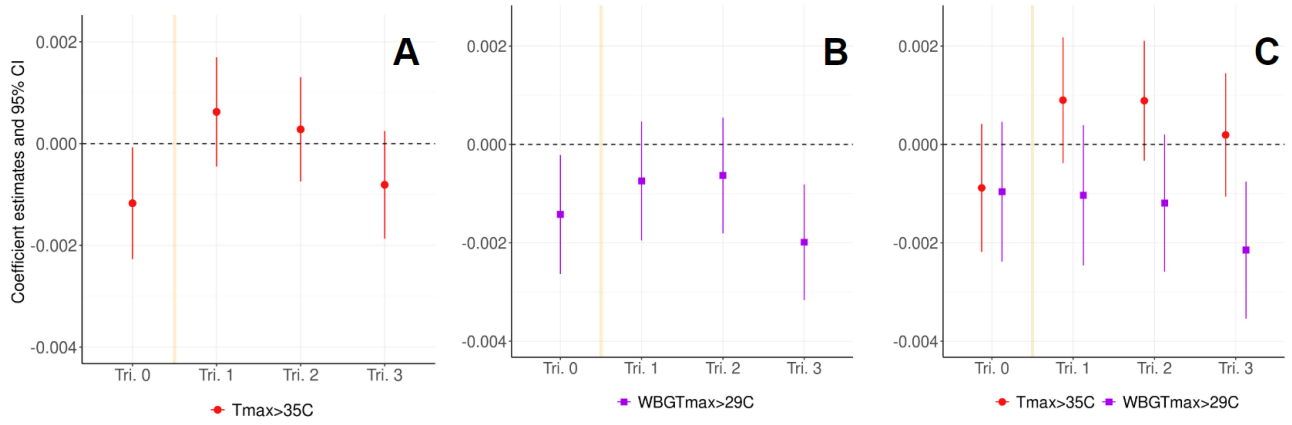

Figure 2. Main effects of heat exposure on HAZ. Coefficients and 95% confidence intervals for the effect of Tmax>35°C (a), WBGTmax>29°C (b), and all heat (c) on HAZ. "Tri. 0" refers to the three-month period before conception, which is represented in each plot with a yellow vertical line. Controls for child's sex, twin status, birth order, birth location, child's age in months, birth month, month of survey, mother's age in years, mother's educational attainment, parity, religion, marital status, and improved toilet access are included in the model but not shown. Fixed effects for cluster and state-by-survey-year are also omitted (see SI Tables 2-4 for regression results).

whereas Panel (c) presents the results from our joint model with both metrics included. In each case, variables for heat exposure from every trimester (0-3) are included among the covariates.

Panel (a) of Figure 2 shows that maximum temperatures above 35°C are associated with reductions in height-for-age when exposure occurs during the three months before conception (or "trimester 0") and the third trimester of pregnancy. We estimate that each additional day with Tmax>35°C decreases the conditional mean of HAZ by 0.001 in the case of pre-conception exposures and 0.0008 for third trimester exposures. Put differently, a one standard deviation increase in the number of hot days leading up to conception would reduce HAZ by an average of 0.017 standard deviations in early childhood, while an equivalent exposure during trimester 3 would result in a reduction of 0.016 standard deviations. The effect in trimester 3 corroborates findings from previous studies that link late-term heat exposure with increased risk of adverse birth outcomes such as pre-term birth and low birth weight[16,35]. The pre-conception effect points to a less well-documented but plausible mechanism related to maternal health at the outset of pregnancy[15]. Meanwhile, heat exposure during trimesters 1 and 2 have no statistically measurable effect on HAZ.

Like Tmax, WBGTmax extremes are associated with lower HAZ in early childhood, particularly when exposure occurs at the beginning or the end of the prenatal year (Panel b). Unlike Tmax, however, hot-humid heat during any trimester is detrimental to child health; all estimated coefficients are negative. Moreover, the negative effects of WBGTmax>29°C on height attainment are larger in magnitude than those of Tmax>35°C. Whereas a one standard deviation increase in days with Tmax>35°C during trimester 3 would lower HAZ by only 1.3% from the sample average (-1.57), an equivalent increase in days with WBGTmax>29°C would imply a 3.7% decrease in HAZ. These effects are also likely to accumulate across trimesters. For example, a child who experienced a one-standard deviation increase in hot-humid days in every trimester would be 7.7% shorter for their age, relative to the sample mean, than a child with average exposure. For Tmax>35°C, the equivalent cumulative effect across trimesters would be only a 1.4% decrease in HAZ.

Finally, we present coefficients from a third model (Panel c) that allows for a more direct comparison of the relative health risks of hot vs hot-humid heat by including all Tmax and WBGTmax exposure variables among the covariates. The results from this model reaffirm that days with WBGTmax>29°C pose a greater threat to child health than days with Tmax>35°C. In fact, after controlling for hot-humid days, exposure to Tmax>35°C has little or no negative effect on child growth. The exception lies in the trimester before conception, where we estimate that each additional day above either heat threshold reduces HAZ by 0.001 (SE=0.0007) standard deviations. Otherwise, all coefficients on HAZ are now positive in the case of Tmax while remaining negative in the case of WBGTmax. While some of the polarization in effect sign may be attributable to the moderate positive correlation between our two heat thresholds, it remains notable the effects of hot-humid extremes remain remarkably consistent with the WBGTmax-only model (Panel b).

To further characterize our main findings, we combine the effects presented in Figure 2 (Panels a and b) with new projections of WBGTmax and Tmax produced by the Climate Hazards Center[38]. These data leverage the same daily 0.05° heat records

used in our main analysis, but they are now perturbed according to four climate change scenarios. Replicating the procedure used in the primary dataset, we link our sample of children to the conditions they would have experienced during their prenatal year under a high-emissions climate change scenario (SSP5-8.5) with 2050 warming (SI Table 1). Because we use each child's unique month, year, and location of birth to identify exposure to extremes, we retain full spatial and temporal variation in the projected data. With the resulting dataset, we calculate the difference between the projected and observed number of extreme days for each trimester for each child. Under the 2050 warming scenario, the average child in our sample is projected to experience approximately 34 days per trimester with WBGTmax$>$29°C and 28 days with Tmax$>$35°C, representing a 54.5% and 47.4% increase in average exposure from our sample mean of 22 days and 19 days, respectively.

Next, we multiply our coefficients on WBGTmax$>$29°C exposure (Fig. 2b) by the projected change in extreme days for each child (SI Table 1) and sum the results across all trimesters. On average, the projected increase in hot-humid heat would imply a decrease HAZ by 0.05 units, suggesting a shift into stunting for any child whose observed HAZ score falls between -1.95 and -2. In total, we calculate that an additional 0.018% (N=3,489) of all children in our dataset would be stunted had their prenatal period occurred under 2050 conditions, a fraction that contains more than 2.2 million children under the age of 5 after applying DHS survey weights. These weights are derived using the United Nations Population Division population estimates from each county at the time of each DHS survey round (Boyle et al., 2022). Using the same logic and corresponding point estimates from our regression of HAZ on Tmax exposure (Fig. 2a), we calculate that increased temperatures under 2050 warming would only have the power to induce stunting in an additional 500,000 children compared to the stunting reflected in the DHS sample. This difference implies that failing to account for the added effect of humidity would lead us to underestimate the vulnerable population by over 1.7 million children. Note that these estimates carry a large degree of uncertainty from several sources, including our coefficient estimates, overall statistical model, and projections of temperature and wet-bulb globe temperature. They should be understood as an imperfect illustration of the relative magnitude of our coefficients on WBGTmax and Tmax rather than a prediction of stunting rates in 2050. Finally, given that population growth is often the largest contributor to rising rates of hot-humid heat exposure in South Asia[25], this approximation may be an underestimate of the true number of children who will be vulnerable to heat-induced stunting in 2050 after accounting for the growing population.

Robustness Checks

We run several tests and additional model specifications to alleviate concerns regarding causality in our main results. First, we replicate all HAZ models using the probability of stunting as the outcome (HAZ $<$ -2) in order to highlight the effects of heat exposure among those in the left tail of the height-for-age distribution (SI Tables 5-7 and SI Fig. 2). We observe the same pattern of effects from these models as from our main HAZ regressions, if somewhat more pronounced. Second, we re-run our main models using higher heat thresholds (Tmax=40°C and WBGTmax=31°C; SI Fig. 3). While the point estimates from these models appear to suggest these hotter conditions are less dangerous than Tmax$>$35°C and WBGTmax$>$29°C, they suffer from a lack of precision given the rarity of these extreme values across much of our study region. These estimates are also likely subject to increases in selection bias as the risk of missed conceptions, pregnancy loss, preterm birth, and stillbirth increase at the highest heat values[16,39,40]. Third, we add a control for total precipitation at the trimester level, as precipitation is correlated with both temperature and humidity. The results from this model, shown in SI Figure 4, remain similar to those in Figure 2. Fourth, we investigate the importance of our primary exposure periods (trimesters 0-3) by adding variables for exposure to WBGTmax$>$29°C during the period 3-6 months before conception ("trimester -1") and the 3 months after birth ("trimester 4"). The new coefficients on hot-humid heat during trimesters -1 and 4 are close to zero whereas those on trimesters 0-3 remain consistent with our main results (SI Fig. 5).

Discussion

Our results indicate that exposure to extreme heat during the year before birth undermines child health, reducing height-for-age for children under the age of five in Bangladesh, India, and Nepal. Compared to temperature alone, exposure to wet-bulb globe temperature extremes is associated with much stronger reductions in height attainment, reflecting a lowered ability to cope with extreme heat during humid conditions. In the third trimester, a one-standard deviation increase in humid heat exposure is seven times more detrimental to height attainment than an equivalent increase in exposure to heat alone, decreasing HAZ by 3.7% and 1.3% relative to the sample mean, respectively. Our point estimates are consistent with previous research on climate-induced stunting. Whereas we find that each additional day in the third trimester with WBGTmax$>$29°C decreases HAZ by 0.002 units, two recent studies find a 0.003 unit decrease in HAZ associated with both (a) each day of delayed monsoon onset in Indonesia and (b) each day with extreme rain in South Asia during the prenatal period[32,41]. The effects we uncover are also notable in magnitude. Combined with new climate projections, our coefficient estimates on WBGTmax imply that more than 2.2 million additional children would have been stunted in our three study countries had they been exposed to levels of heat and humidity expected by 2050 under a high-emissions climate change scenario. When we define future heat exposure using Tmax, we undercount this effect by approximately 1.7 million children.

Moreover, our results corroborate previous scholars' assertations that the timing of exposure plays a critical role in determining the long-term impacts of climate shocks on child health[42]. The adverse effects of heat exposure during trimester 3 documented above align with existing epidemiological evidence that heat stress and dehydration towards the end of gestation can induce labor prematurely, thereby increasing rates of pre-term birth and associated health risk for mothers and babies[16,35]. We also find consistent and suggestive evidence that exposure to hot-humid extremes during the three months before conception undermines health. This added vulnerability during the pre-conception period suggests that maternal health status at the outset of pregnancy can influence children's outcomes at birth and beyond. Indeed, previous research has linked extreme heat during this period with decreases in both conception rates[39] and birth weights[43]. This result is also in alignment with a recent large-scale study that finds that the well-being of reproductive-age women in low- and middle-income countries is sensitive to temperature shocks across a wide range of outcomes, including nutritional health and fertility behavior[7]. Though more research is needed to illuminate the exact mechanisms linking extreme heat before conception with height attainment after birth, the physiological consequences of extreme heat exposure during the weeks leading up to and following conception may set the most socially vulnerable children on a path towards slower growth.

There are several limitations to our data and specification choices that could influence the analysis and findings presented here. First, the DHS variables for children's age, month and year of birth, and length of residence in their current household rely on respondents' recall, and therefore may be subject to measurement error based on flawed memory and approximations (see[44] and[45] for discussions on age heaping in the DHS). This potential measurement error may then affect our identification of heat exposure, which is based on exact month of birth and location of each mother within her cluster of residence during the year before giving birth. We are also unable to define exact trimester of exposure given that the DHS lacks complete and reliable information on day of birth and length of gestation, meaning that we necessarily take on some measurement error at the sub-monthly scale in our variables for the total number of hot days per trimester. Data limitations further inhibit our ability to identify the mechanisms that drive the relationship between heat exposure and HAZ that we observe here. These data alone lack the specificity and power needed to identify or eliminate precise mechanisms. Additionally, our results may be sensitive to the specification of heat thresholds and the combination of data from multiple countries, though the fixed effects in our models account for the vast majority of cross-country differences. See SI Fig. 3 for a version of our main models using higher thresholds for Tmax (40°C) and WBGTmax (31°C). Frequency and intensity of exposure to extreme heat and humidity are highly variable across South Asia (Fig. 1), meaning that days above our heat thresholds (Tmax>35°C and WBGTmax>29°C) are more common in some communities than others, influencing the precision of our estimates in cooler and drier regions. Future research should take this variability into account when identifying critical thresholds for heat exposure.

Taken together, our results suggest that the long-run health consequences of extreme heat and humidity during the prenatal period represent a vastly underappreciated cost of climate change. Exposure to hot-humid extremes continues to accelerate in these regions, threatening to undermine ongoing efforts to improve child health and economic outcomes. Jobs, farms, cities and people tend to be located along densely populated tropical river valleys and coastlines, where it is frequently very humid and likely to see increases in both heat and humidity in the coming decades. South Asian humid heat extremes, therefore, tend to follow population distributions, amplifying risk (SI Fig. 1). Our findings point to an opportunity to protect child and maternal health from climate extremes by enhancing warning systems and medical support for pregnant people during periods of extreme heat and humidity.

Methods

Heat Data

We extract daily records of maximum temperature (Tmax) and maximum wet-bulb globe temperature (WBGTmax) for each DHS survey location using the Climate Hazards Center InfraRed Temperature with Stations data (CHIRTS), a high-resolution gridded temperature product created by the Climate Hazards Center at the University of California, Santa Barbara. Specifically developed to perform well in poorly monitored regions of the Global South, CHIRTS is the most robust temperature product available to date, improving upon previous datasets by combining satellite imagery with reanalysis data and in-situ station observations to produce accurate, fine-scale (0.05° resolution) temperature estimates in otherwise data-poor regions[17,18]. This product is particularly crucial in enabling our use of WBGTmax as a key explanatory variable. In addition to ambient air temperature, WBGTmax contains information about relative humidity, wind speed, and sunlight intensity, all of which influence the body's ability to dissipate heat[46]. In CHIRTS WBGTmax, these influences are parameterized as a function of heat index (HI) (Eq. 1). Detailed validation studies can be found in[18] and the supplemental material in[25]. While there are different means of quantifying humid heat extremes, all approaches face severe data limitations in India, Bangladesh and Nepal, where monthly[17] and daily[18] temperature observations are very limited. Following Bernard and Iheanacho[46], WBGTmax is calculated as follows:

$$WBGT_{max}(^{\circ}C) = -0.0034 * HI^2_{max}(^{\circ}F) + 0.96 * HI_{max}(^{\circ}F) - 34 \quad (1)$$

where HImax is calculated in accordance with guidelines from the National Oceanic and Atmospheric Administration using daily temperature data from CHIRTS and daily relative humidity from down-scaled reanalysis data from version 5 of the European Centre for Medium-Range Weather Forecasts Reanalysis (ERA5) (see Materials and Methods in[25]).

Defining Exposure

We define extreme heat days using one biologically-relevant threshold for each variable: 35°C for Tmax and 29°C for WBGTmax. Though some existing studies use relative thresholds (usually based on percentiles of local temperature distributions or deviations from a historical mean, e.g.[32], we argue that absolute metrics are better suited for capturing the physiological mechanisms that link extreme heat and maternal and infant health in the prenatal period[35]. Ambient air temperatures exceeding 35°C have been consistently shown to increase the risk of heat-induced morbidity and mortality[4,47], and wet-bulb globe temperatures above 29°C are classified as hazardous for unacclimatized people at low metabolic rates (125 to 235 W) by the US Occupational Safety and Health Administration[48] and the International Standards Organization[49]. Furthermore, days with Tmax>35°C and WBGTmax>29°C occur with nearly equal frequency (21% and 20%, respectively) in our sample, making them comparable in terms of exposure and acclimatization within the population (SI Table 1).

We use information on month, year, and location of birth from the Demographic and Health Surveys to define prenatal heat exposure for each child in our sample. For each day in the CHIRTS observational period (1983-2016), we extract a spatial mean of all pixels that lie within a 10-kilometer buffer around each DHS survey location. This buffer accounts for the random displacement of surveyed locations performed by the DHS to protect respondents' privacy. Though scholars have shown that alternative geospatial approaches are sometimes better suited to accounting for such displacement in population-environment research[50], this buffer technique remains robust when dealing with temperature variables. We then use each child's month and year of birth to count the number of days with Tmax>35°C and WBGTmax>29°C during each trimester in the year before birth. In addition to trimesters 1-3, during which gestation takes place, we also observe heat exposure during "trimester 0," which spans the three months preceding conception. Aside from the importance of proper maternal nutrition and health leading up to pregnancy[42], extreme heat during this period has been shown reduce conceptions[39,51] and decrease the birth weights of babies born 9-12 months later[15], suggesting that these pre-conception months are important determinants of health trajectories for mothers and babies throughout pregnancy and beyond. Because the exact day of birth is rarely recorded and subject to recall error, we mark the start and end of each trimester using the 15th day of a given month. Though consistent across observations, this strategy means that a fraction of hot days is necessarily mis-assigned for any child not born on the 15th of the month. Without information on length of gestation, we also assume that each pregnancy reached a full nine months. Finally, to protect our identification of individual-level heat exposure, we exclude any respondents who moved residences at any point during the child's life or prenatal year, as well as those lacking data on migration history altogether (N=120,608).

Figure 3 depicts the distribution of Tmax and WBGTmax, and the orange lines denote our final biologically-relevant heat thresholds for each. While both distributions are left-skewed, this feature is particularly pronounced for WBGTmax. The mode of both distributions falls around 30°C, although Panel (b) also shows a heaping of WBGTmax values around 22°C. For WBGT, this means that the most typical humid heat values are already potentially dangerous. This feature may reflect a seasonal shift in WBGTmax, or else regional differences in heat and humidity across the subcontinent. In our study locations, 72.1% of days from 1983-2016 did not exceed either heat threshold, 12.5% exceeded both, 7.4% were extreme by Tmax standards only, and 8.1% were extreme according only to WBGTmax. See Figure 1 for an understanding of how each of these four categories are distributed geographically across the region. The 15.5% of days that exceed one threshold but not the other reflect the complex construction of wet-bulb globe temperature.

Child Health Data

We leverage data on child growth trajectories, demographic characteristics, and village locations from the Demographic and Health Surveys. The DHS collect detailed, representative data on anthropometrics and demographics in countries that often lack adequate local and national health data. We access the DHS child questionnaires in a user–friendly format from IPUMS[52]. Our sample includes 0- to 5-year-old children from all IPUMS-DHS surveys in Bangladesh, India, and Nepal that contain both child anthropometric records (i.e., height and weight, measured at the time of survey) and geographic identifiers at the DHS' smallest spatial unit. These spatial units are referred to as "clusters" and are approximately the size of a single rural village or urban city block. In total, our final dataset contains 29,357 clusters with 198,710 observations from the following DHS rounds: Bangladesh 1999-2000 (N=4,260), Bangladesh 2004 (N=4,552), Bangladesh 2007 (N=3,951), India 2015- 2016 (N=174,668), Nepal 2001 (N=5,230), Nepal 2006 (N=4,229), and Nepal 2016 (N=1,820). Note that while DHS round-specific sampling weights help to balance unequal sample sizes between rounds, the majority of our observations are from India 2015-2016, an El Niño year with exceptionally warm Indian air temperatures[26].

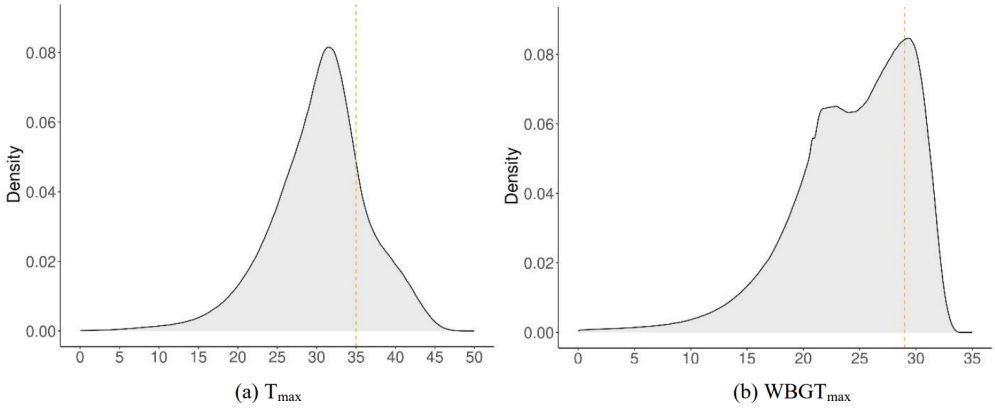

Figure 3. Density curves of daily Tmax (Panel a) and WBGTmax (Panel b) in all DHS clusters (1983-2016). Orange dotted lines mark our biologically-relevant thresholds (Tmax=35°C, WBGTmax=29°C).

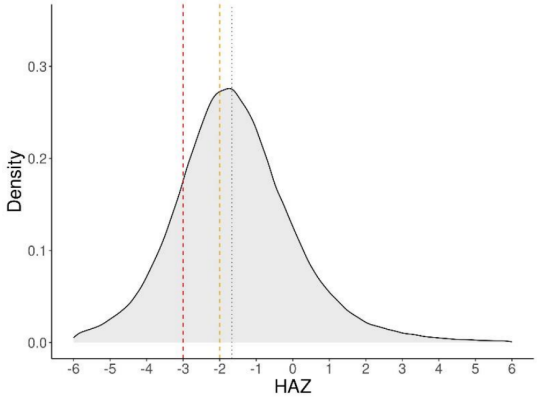

Figure 4. Density curve of HAZ in DHS sample. Black dotted line marks the sample median. Orange and red dashed lines mark the WHO thresholds for stunting and severe stunting, respectively.

Our outcome measure for child height is a continuous Z-score of height-for-age ratio, which is the basis for defining stunting (HAZ<-2)[53]. This anthropometric measurement is observed at the time of survey only. We include stunting as an additional outcome in the Supplemental Information (see SI Tables 5-6 and SI Figure 2). Figure 4 presents the distribution of HAZ in our sample, with markers for the thresholds of stunting and severe stunting as well as the sample median. The height-for-age Z-score for each child is calculated relative to the median height among a globally-representative population of children of the same age and sex[53], and ranges from -6 to 6 standard deviations. Strikingly, the sample median falls close to HAZ = -2, meaning that nearly 50% of all 0 to 5 year-olds in our sample were stunted at the time of survey. In addition to HAZ, we employ a number of key demographic variables related to socioeconomic status, child development, and health. See Estimation Strategy for a full list of covariates and SI Table 1 for summary statistics.

Estimation Strategy

We employ two main models of child height. First, we regress height attainment on trimester-level exposure to either Tmax>35°C or WBGTmax>29°C, along with our full suite of demographic controls and cluster, month, and state by survey-year fixed effects (Equation 2). We run this model twice—once for Tmax and once for WBGTmax extremes—and include covariates for exposure in all trimesters (0-3) each time. See SI Figure 5 for the results of an alternative model that includes exposure during the 3-month period before trimester 0 as well as the 3 months after birth. Our first regression is estimated as follows:

$$Y_{ij} = \beta_0 + \sum_{\tau=0}^{\tau=3} \beta_{1_\tau} D_{h\tau ij} + \beta_2 X_{ij} + \mu_j + \gamma_{ts} + \varepsilon_{ij} \quad (2)$$

where Y_{ij} is the HAZ score for child i in DHS cluster j. As a supplement, we also run Eq. 2 as a linear probability model with stunting as the outcome (see SI Tables 5-7 and SI Fig. 2). β_1 captures the effect of a marginal increase in the number of days ($D_{h\tau ij}$) that the heat metric D exceeded threshold h (corresponding to Tmax>35°C or WBGTmax>29°C) during trimester τ for child i in cluster j on our prediction of the conditional mean of HAZ, holding other covariates constant. See SI Figure 4 for a version of Eq. (2) that adds a control for total precipitation at the trimester level. The X_{ij} term is a comprehensive set of controls at the child, maternal, and household levels. These include the child's sex, twin status, birth order, and birth location (health clinic or other); mother's educational attainment, parity, religion, and marital status; and an indicator variable for whether the household has access to an improved toilet (defined using DHS classifications). A set of individual-level controls for child's age in months, birth month, mother's age in years, and month of DHS survey is also captured in X_{ij} to account for nonlinearity in height-for-age across age groups and seasonal variation in nutritional status. We include cluster fixed effects (μ_j), which control for latent and time-invariant community-level characteristics that influence children's heights. Finally, we include state-by-survey-year fixed effects (γ_{ts}) to flexibly capture macro-level trends in child health and nutrition over time. With these robust fixed effects, the remaining variation comes from within-cluster differences in prenatal heat exposure among individuals, based on the varying ages of children in our sample. Specifically, we compare children with similar sociodemographic characteristics who were born in the same cluster and calendar month but different years within the five-year period captured retrospectively by a given DHS survey. We assume that this remaining variation in heat exposure is random after controlling for spatial, temporal, and socioeconomic factors. We further include DHS sampling weights to account for the clustered sampling design and unequal sample sizes across countries and survey years, and we cluster standard errors at the DHS cluster level.

Our second model closely mirrors Eq. (2), but now includes covariates for trimester-level exposure to both Tmax>35°C ($\theta_{\tau ij}$) and WBGTmax>29°C ($\omega_{\tau ij}$) so as to create a more direct comparison of the relative health effects of each heat type (Equation 3).

$$Y_{ij} = \beta_0 + \sum_{\tau=0}^{\tau=3} \beta_{1_\tau} \theta_{\tau ij} + \sum_{\tau=0}^{\tau=3} \beta_{2_\tau} \omega_{\tau ij} + \beta_3 X_{ij} + \mu_j + \gamma_{ts} + \varepsilon_{ij} \quad (3)$$

Now, β_1 should represents the change in the conditional mean of the outcome given a marginal increase in the number of days where Tmax exceeded 35°C during trimester τ for child i living in cluster j after holding hot-humid heat exposure constant, in addition to the other covariates. Likewise, β_2 now reports the marginal effect of trimester-level exposure to days with WBGTmax>29°C, unconfounded by Tmax. The excluded category therefore encompasses all days that do not surpass either heat threshold. The outcome variable, controls, and fixed effect terms remain unchanged from Eq. (2). See SI Table 7 and SI Fig. 2 for a version of Eq. 3 with the probability of stunting as the outcome.

Data Availability

CHIRTSdaily gridded temperature data, wet-bulb globe temperature data, and CHC-CMIP6 projection data are publicly available from the Climate Hazards Center (https://data.chc.ucsb.edu/products/CHIRTSdaily/). The Demographic and Health Survey data used for this study are available after a simple application at www.dhsprogram.com and can be easily accessed through IPUMS (https://www.idhsdata.org/idhs/).

Code Availability

Analyses were performed in R, a free and open-source data management software. To the extent possible given data privacy limitations associated with the Demographic and Health Surveys, all code will be made publicly available via GitHub upon publication.

References

1. IPCC. AR6 Synthesis Report: Climate Change 2023. Tech. Rep. (2023).
2. Hajat, S., Armstrong, B. G., Gouveia, N. & Wilkinson, P. Mortality Displacement of Heat-Related Deaths: A Comparison of Delhi, São Paulo, and London. *Epidemiology* **16**, 613–620 (2005). Publisher: Lippincott Williams & Wilkins.
3. Burgess, R., Deschenes, O., Donaldson, D. & Greenstone, M. The unequal effects of weather and climate change: Evidence from mortality in India. *Cambridge, United States: Mass. Inst. Technol. Dep. Econ. Manuscr.* (2014).

4. Deschenes, O. Temperature, human health, and adaptation: A review of the empirical literature. **46**, 606–619, DOI: 10.1016/j.eneco.2013.10.013 (2014-11-01).

5. Nerbass, F. B. *et al.* Occupational Heat Stress and Kidney Health: From Farms to Factories. *Kidney Int. Reports* **2**, 998–1008, DOI: 10.1016/j.ekir.2017.08.012 (2017).

6. Smith, D. G. What Extreme Heat Does to Your Body. *The New York Times* (2023).

7. Gray, C. & Thiede, B. Temperature anomalies undermind the health of reproductive-age women in low- and middle-income countries. *Proc. Natl. Acad. Sci.* **121** (2024).

8. Parsons, K. *Human Thermal Environments: The Effects of Hot, Moderate, and Cold Environments on Human Health, Comfort and Performance, Second Edition* (CRC Press, London, 2002), 2 edn.

9. Parsons, K. Heat stress standard ISO 7243 and its global application. **44**, 368–379, DOI: 10.2486/indhealth.44.368 (2006).

10. Budd, G. M. Wet-bulb globe temperature (wbgt)—its history and its limitations. *J. science medicine sport* **11**, 20–32 (2008).

11. Im, E.-S., Pal, J. S. & Eltahir, E. A. B. Deadly heat waves projected in the densely populated agricultural regions of South Asia. *Sci. Adv.* **3**, e1603322, DOI: 10.1126/sciadv.1603322 (2017). Publisher: American Association for the Advancement of Science.

12. Carolan-Olah, M. & Frankowska, D. High environmental temperature and preterm birth: a review of the evidence. *Midwifery* **30**, 50–59, DOI: 10.1016/j.midw.2013.01.011 (2014).

13. Zhang, Y., Yu, C. & Wang, L. Temperature exposure during pregnancy and birth outcomes: An updated systematic review of epidemiological evidence. *Environ. Pollut.* **225**, 700–712, DOI: 10.1016/j.envpol.2017.02.066 (2017).

14. Basu, R., Rau, R., Pearson, D. & Malig, B. Temperature and Term Low Birth Weight in California. *Am. J. Epidemiol.* **187**, 2306–2314, DOI: 10.1093/aje/kwy116 (2018).

15. Grace, K., Davenport, F., Hanson, H., Funk, C. & Shukla, S. Linking climate change and health outcomes: Examining the relationship between temperature, precipitation and birth weight in africa. **35**, 125–137, DOI: 10.1016/j.gloenvcha.2015.06.010 (2015-11-01).

16. Davenport, F., Dorélien, A. & Grace, K. Investigating the linkages between pregnancy outcomes and climate in sub-saharan africa. **41**, 397–421, DOI: 10.1007/s11111-020-00342-w (2020-06-01).

17. Funk, C. *et al.* A high-resolution 1983–2016 tmax climate data record based on infrared temperatures and stations by the climate hazard center. **32**, 5639–5658, DOI: 10.1175/JCLI-D-18-0698.1 (2019-09-01). Publisher: American Meteorological Society Section: Journal of Climate.

18. Verdin, A. *et al.* Development and validation of the CHIRTS-daily quasi-global high-resolution daily temperature data set. **7**, 303, DOI: 10.1038/s41597-020-00643-7 (2020-09-14).

19. Vecellio, D. J., Kong, Q., Kenney, W. L. & Huber, M. Greatly enhanced risk to humans as a consequence of empirically determined lower moist heat stress tolerance. *Proc. Natl. Acad. Sci.* **120**, e2305427120, DOI: 10.1073/pnas.2305427120 (2023). Publisher: Proceedings of the National Academy of Sciences.

20. Rayco-Solon, P., Fulford, A. J. & Prentice, A. M. Maternal preconceptional weight and gestational length. *Am. J. Obstet. Gynecol.* **192**, 1133–1136, DOI: 10.1016/j.ajog.2004.10.636 (2005).

21. Almond, D. & Currie, J. Killing me softly: The fetal origins hypothesis. **25**, 153–172, DOI: 10.1257/jep.25.3.153 (2011-09).

22. Ramakrishnan, U., Grant, F., Goldenberg, T., Zongrone, A. & Martorell, R. Effect of Women's Nutrition before and during Early Pregnancy on Maternal and Infant Outcomes: A Systematic Review. *Paediatr. Perinat. Epidemiol.* **26**, 285–301, DOI: 10.1111/j.1365-3016.2012.01281.x (2012). _eprint: https://onlinelibrary.wiley.com/doi/pdf/10.1111/j.1365-3016.2012.01281.x.

23. Nobles, J. & Hamoudi, A. Detecting the Effects of Early-Life Exposures: Why Fecundity Matters. *Popul. Res. Policy Rev.* **38**, 783–809, DOI: 10.1007/s11113-019-09562-x (2019).

24. Pachauri, R. K. *et al. Climate Change 2014: Synthesis Report. Contribution of Working Groups I, II and III to the Fifth Assessment Report of the Intergovernmental Panel on Climate Change* (IPCC, 2014). Pages: 151 Publication Title: EPIC3Geneva, Switzerland, IPCC, 151 p., pp. 151, ISBN: 978-92-9169-143-2.

25. Tuholske, C. *et al.* Global urban population exposure to extreme heat. **118**, e2024792118, DOI: 10.1073/pnas.2024792118 (2021-10-12). Publisher: Proceedings of the National Academy of Sciences.

26. Funk, C. C. *Drought, Flood, Fire: How Climate Change Contributes to Catastrophes* (Cambridge University Press, 2021). Google-Books-ID: MdEnEAAAQBAJ.

27. Matthews, T. K. R., Wilby, R. L. & Murphy, C. Communicating the deadly consequences of global warming for human heat stress. *Proc. Natl. Acad. Sci.* **114**, 3861–3866, DOI: 10.1073/pnas.1617526114 (2017). Publisher: Proceedings of the National Academy of Sciences.

28. UNICEF. Undernourished and overlooked: A global nutrition crisis in adolescent girls and women. *UNICEF Child Nutr. Rep. Series, 2022* (2023).

29. Shively, G., Sununtnasuk, C. & Brown, M. Environmental variability and child growth in nepal. **35**, 37–51, DOI: 10.1016/j.healthplace.2015.06.008 (2015-09).

30. Spears, D. Exposure to open defecation can account for the indian enigma of child height. **146**, DOI: https://doi.org/10.1016/j.jdeveco.2018.08.003 (2020).

31. Brown, C., Kandpal, E., Lee, J. & Williams, A. Unequal households or communities?: Decomposing the inequality in nutritional status in south asia, DOI: 10.1596/1813-9450-10009 (2022-04).

32. McMahon, K. & Gray, C. Climate change, social vulnerability and child nutrition in south asia. **71**, 102414, DOI: 10.1016/j.gloenvcha.2021.102414 (2021-11-01).

33. Burke, M., Hsiang, S. M. & Miguel, E. Global non-linear effect of temperature on economic production. **527**, 235–239, DOI: 10.1038/nature15725 (2015-11).

34. Davenport, F., Grace, K., Funk, C. & Shukla, S. Child health outcomes in sub-saharan africa: A comparison of changes in climate and socio-economic factors. **46**, 72–87, DOI: 10.1016/j.gloenvcha.2017.04.009 (2017-09).

35. Randell, H., Gray, C. & Grace, K. Stunted from the start: Early life weather conditions and child undernutrition in ethiopia. **261**, 113234, DOI: 10.1016/j.socscimed.2020.113234 (2020-09).

36. Deschênes, O., Greenstone, M. & Guryan, J. Climate Change and Birth Weight. *Am. Econ. Rev.* **99**, 211–217, DOI: 10.1257/aer.99.2.211 (2009).

37. Guo, T. *et al.* The association between ambient temperature and the risk of preterm birth in China. *Sci. The Total. Environ.* **613-614**, 439–446, DOI: 10.1016/j.scitotenv.2017.09.104 (2018).

38. Williams, E., Funk, C., Peterson, P. & Tuholske, C. High resolution climate change observations and projections for the evaluation of heat-related extremes. *Sci. Data* **11**, 261 (2024).

39. Barreca, A., Deschenes, O. & Guldi, M. Maybe next month? temperature shocks and dynamic adjustments in birth rates. *Demography* **55**, 1269–1293 (2018).

40. Ward, A. *et al.* The impact of heat exposure on reduced gestational age in pregnant women in North Carolina, 2011–2015. *Int. J. Biometeorol.* **63**, 1611–1620, DOI: 10.1007/s00484-019-01773-3 (2019).

41. Thiede, B. C. & Gray, C. Climate exposures and child undernutrition: Evidence from indonesia. **265**, 113298, DOI: 10.1016/j.socscimed.2020.113298 (2020-11).

42. Grace, K. *et al.* Exploring strategies for investigating the mechanisms linking climate and individual-level child health outcomes: An analysis of birth weight in mali. **58**, 499–526, DOI: 10.1215/00703370-8977484 (2021-04-01).

43. Grace, K. & Nagle, N. N. Using high-resolution remotely sensed data to examine the relationship between agriculture and fertility in mali. **67**, 641–654, DOI: 10.1080/00330124.2015.1032899 (2015-10-02). Publisher: Routledge _eprint: https://doi.org/10.1080/00330124.2015.1032899.

44. Lyons-Amos, M. & Stones, T. Trends in Demographic and Health Survey data quality: an analysis of age heaping over time in 34 countries in Sub Saharan Africa between 1987 and 2015. *BMC Res. Notes* **10**, 760, DOI: 10.1186/s13104-017-3091-x (2017).

45. Singh, M., Kashyap, G. C. & Bango, M. Age heaping among individuals in selected South Asian countries: evidence from Demographic and Health Surveys. *J. Biosoc. Sci.* **54**, 725–734, DOI: 10.1017/S0021932021000249 (2022). Publisher: Cambridge University Press.

46. Bernard, T. E. & Iheanacho, I. Heat index and adjusted temperature as surrogates for wet bulb globe temperature to screen for occupational heat stress. *J. Occup. Environ. Hyg.* **12**, 323–333 (2015).

47. Barreca, A., Clay, K., Deschenes, O., Greenstone, M. & Shapiro, J. S. Adapting to climate change: The remarkable decline in the US temperature-mortality relationship over the twentieth century. **124**, 105–159, DOI: 10.1086/684582 (2016-02). Publisher: The University of Chicago Press.

48. OSHA. Osha technical manual, section iii, chapter 4. heat stress. (2017).

49. ISO. Ergonomics of the thermal environment—assessment of heat stress using the wbgt (wet bulb globe temperature) index. *Int Org Standard Geneva Switz.* (2017).

50. Grace, K. *et al.* Integrating environmental context into dhs analysis while protecting participant confidentiality: A new remote sensing method. *Popul. development review* **45**, 197 (2019).

51. Lam, D. A. & Miron, J. A. The effects of temperature on human fertility. *Demography* **33**, 291–305, DOI: 10.2307/2061762 (1996).

52. Boyle, E. H., King, M. & Sobek, M. IPUMS -Demographic and Health Surveys: Version 9 [dataset] (2022).

53. WHO. *WHO child growth standards.* (World Health Organization, 2006).

Acknowledgements

We thank participants at the annual meetings of the Graduate Climate Conference, PAA, the All-UC Demography Conference, and AGU for their feedback in 2022 and 2023. KM was supported by the NSF Graduate Research Fellowship Program and the Chancellor's Fellowship from UC Santa Barbara.

Author contributions statement

K.M., K.B., S.S., and C.F. conceived the analysis, K.M. conducted the analysis, K.M. analysed the results. All authors reviewed the manuscript.

Additional information

Competing interests

The authors declare no competing interests.